CYP2E1 in the Human Retinal Pigment Epithelium: Expression, Activity, and Induction by Ethanol

Natalia Martinez-Gil,[1] Miguel Flores-Bellver,[2] Sandra Atienzar-Aroca,[1] Daniel Lopez-Malo,[1] Alba C. Urdaneta,[1] Javier Sancho-Pelluz,[1] Cristina Peris-Martínez,[1] Luis Bonet-Ponce,[1] Francisco J. Romero,[1] and Jorge M. Barcia[1]

[1]School of Medicine, Universidad Catolica de Valencia San Vicente Martir, Valencia, Spain
[2]The Wilmer Eye Institute, Johns Hopkins Hospital, Baltimore, Maryland, United States

Correspondence: Francisco J. Romero, School of Medicine, Universidad Catolica de Valencia San Vicente Martir, Quevedo 2, 46001-Valencia, Spain; fj.romero@ucv.es.

NM-G and MF-B contributed equally to the work presented here and should therefore be regarded as equivalent authors.

Submitted: December 19, 2014
Accepted: September 12, 2015

Citation: Martinez-Gil N, Flores-Bellver M, Atienzar-Aroca S, et al. CYP2E1 in the human retinal pigment epithelium: expression, activity, and induction by ethanol. *Invest Ophthalmol Vis Sci*. 2015;56:6855–6863. DOI:10.1167/iovs.14-16291

Purpose. Cytochrome p450 2E1 (CYP2E1) is a detoxifying enzyme with particular affinity for ethanol (EtOH) expressed in several tissues. Although CYP2E1 has been identified in human RPE, nothing is known about its metabolic activity. Expression of CYP2E1 and activity after EtOH exposure have been studied in human RPE and ARPE-19 cells.

Methods. Ethanol-induced CYP2E1 mRNA expression was analyzed by RT-PCR and quantitative PCR (qPCR) from human donor RPE as well as from ARPE-19 cells. Expression of CYP2E1 protein was determined by Western blot. Cytoplasmic CYP2E1 location also was demonstrated by immunocytochemistry. Cell viability was studied by the colorimetric assay XTT after EtOH treatment. Diallyl sulfide (DAS) was used to inhibit CYP2E1 activity. The microsomal CYP2E1 activity assay was determined by quantification of 4-nitrocatechol (4NC) formation through HPLC.

Results. Relevant CYP2E1 mRNA levels are present in human RPE. Ethanol augmented the formation of reactive oxygen species (ROS) in ARPE-19 cells. Expression of CYP2E1 mRNA, CYP2E1 protein activity, and ROS production were induced by ethanol in a concentration-dependent manner. Interestingly, the treatment with DAS reduced all the aforementioned increased values. The presence of CYP2E1 in both hRPE and ARPE-19 cells reinforces the protective role of the RPE and strongly suggests additional roles for CYP2E1 related to vision.

Keywords: retinal pigment epithelium, ethanol, CYP2E1

Ethanol (EtOH)–related health problems are a major concern worldwide. Ethanol metabolism produces reactive oxygen species (ROS) and increased EtOH catabolic activity implies higher ROS production,[1–3] promoting tissue damage.[4] The main target of EtOH-induced alterations is the hepatic tissue. Ethanol exposure also causes long-term damage on the central nervous system (CNS), including cognitive effects, such as learning and memory impairments.[5,6] Ethanol is metabolized mainly by oxidative pathways leading to free radical production that negatively affects nervous tissue.[7–10] A minimal nonoxidative EtOH metabolic pathway that produces fatty acid ethyl ester and phosphatidyl ethanol is present secondarily.[11]

Previous observations from our group indicate that chronic EtOH exposure increases oxidative stress in the rat retina accompanied by decreased b-wave amplitude.[12] Interestingly, the addition of Ebselen (an antioxidant selenocompound) normalizes the oxidative misbalance and restores the aforementioned EtOH-induced b-wave impairment.[13]

Recent data demonstrated that EtOH induces autophagy and mitochondrial alterations, ROS generation, and lipid peroxidation in ARPE-19 cells, producing accumulation of 4-hydroxynonenal (HNE) aggregates that is toxic for cells.[14] These results posed the question whether EtOH is significantly metabolized in the retina, and if this metabolism could generate a direct EtOH-related damage.[14]

Cytochrome P450 is a family of enzymes involved in the oxidative metabolism of endogenous and xenobiotic products.[15–17] The cytochrome p450 2E1 (CYP2E1) isoform is involved specifically in EtOH oxidation. It has more affinity for EtOH than alcohol dehydrogenase (ADH).[18] In fact, CYP2E1 assumes an important role in metabolizing EtOH, being considered as a major component of the microsomal EtOH-oxidizing system (MEOS).[19,20] Briefly, MEOS is a network of vesicles from the endoplasmic reticulum that aid in EtOH metabolism in the liver. High blood EtOH levels, observed after chronic EtOH exposure, induce CYP2E1 expression in the liver.[21] Despite the fact that EtOH is catabolized mostly in the liver, the presence of CYP2E1 in other tissues reinforces the possibility of an extrahepatic EtOH tissue metabolism.[22–24]

Due to its location, between the photoreceptors and choroid, the RPE takes part in the blood–retina barrier[25] and, presumably, would be the first retinal cell layer directly exposed to circulating EtOH. The RPE has an important role in photoreceptor maintenance and nutrient regulation[26–31] and has detoxifying properties through expression of CYP2E1 isoforms that are involved in drug metabolizing enzyme synthesis.[32–34]

The presence of a cytochrome P450 in the retina was reported in bovine RPE,[35] and identified later as the CYP1A1 isoform.[33] Nakamura et al.[36] identified several cytochrome P450 enzymes, among them CYP2E1, in the rat ocular tissue, including the RPE. Even though, the major CYP450 isoforms expressed in ARPE-19 cells are CYP1B1 and CYP4V2, other forms such as CYP2E1, CYP2J2, and CYP3A4, are weakly expressed (7 times less than CYP4V2).[32] Despite the fact that

ADH and 11-*cis*-retinol dehydrogenase (RDH5), present in RPE, also metabolize EtOH,[37–39] the exclusive role of CYP2E1 in the oxidation of EtOH (producing ROS) is so relevant that it deserves to be studied apart. The role of RPE in drug and/or EtOH metabolism has been considered quantitatively irrelevant, in view of the small cytochrome P450-mRNA expression found in the eye (less than 1% of cytochrome P450-mRNA expression) compared to the liver.[40] However, the exposure of retinal tissue to high and continuous EtOH concentrations may induce CYP2E1 expression, which would provide new insights into EtOH metabolism and toxicity.

The presence of CYP2E1 in RPE may have a relevant role in EtOH metabolism and eventually in retinal alterations. This work focuses on the characterization of the CYP2E1 isoform in ARPE-19 and human RPE cells, in response to EtOH challenge supporting the hypothesis of local EtOH metabolism.

Materials and Methods

Cell Culture and Treatments

Human RPE (hRPE) cell line ARPE-19 was cultured according to supplier's protocol (American Type Culture Collection [ATCC], Barcelona, Spain). Cells were cultured in Dulbecco's modified Eagle's medium/nutrient mixture F12 (DMEM/F12; Invitrogen, Grand Island, NY, USA) supplemented with 5 mM HEPES buffer, 7.5% $NaHCO_3$, 10% fetal bovine serum (FBS), and 1% penicillin/streptomycin, and were maintained at 37°C and 5% CO_2. Cells were used from passages 18 to 20 and cultured in p100 culture well plates at a seeding density of 1×10^6 cells/cm^2. After 2 days, ARPE-19 cells were treated for 24 hours at different EtOH (Biosolve, Valkenswaard, The Netherlands) concentrations: 200, 400, 600, 800, 1000, or 1200 mM, within fresh medium.

For CYP2E1 Inhibition, Diallyl sulfide (DAS; Santa Cruz Biotechnology, Santa Cruz, CA, USA), a known selective CYP2E1 inhibitor, was added (20 mM in dimethyl sulfoxide [DMSO], 0.1% in all samples) to the culture media without FBS.

Human hepatocellular liver carcinoma (HepG2) cell line was donated generously from the laboratory of Jose Carlos Fernandez-Checa, PhD (IDIBAPS, Barcelona, Spain), and cultured according to supplier's protocol (ATCC).

Human RPE was obtained from human donors at the Fundación Oftalmológica del Mediterráneo (FOM;, Valencia, Spain) according with the Spanish regulations for the handling of human samples. Human RPE cells were isolated by collagenase and trypsin treatment as described previously.[41] Briefly, after removal of the neural retina, sheets of RPE cells were washed with sterile PBS and then incubated with 1% collagenase solution at 37°C and 5% CO_2 for 20 minutes. Then, the cells were incubated with trypsin solution in the same conditions as above for 10 minutes. Finally, cells were recovered by centrifugation and seeded in the same conditions used for ARPE-19 cells. Cells were used from passages 2 to 4. In these passages, cells maintained typical hexagonal morphology, did not lose pigmentation, and all were positively labeled with RPE65 (specific RPE marker).

Cell Viability

The sodium 3′-[1-phenylaminocarbonyl-3,4-tetrazolium]-bis (4-methoxy-6-nitro) benzene sulfonic acid hydrate test (XTT; Cell Proliferation Kit II; Roche, Mannheim, Germany) was used to determine cell viability as mitochondrial activity. The ARPE-19 and hRPE cells were seeded at 6×10^3 cells per well in a 96-well cell culture plate and grown to confluence for 24 hours. Cells were treated with 200, 400, 600, 800, 1000, or 1200 mM EtOH and 20 mM DAS for 24 hours. A final XTT concentration of 0.3 mg/mL was added to each well and incubated for 8 hours at 37°C in 5% CO_2. Subsequently, absorbance was read at 550 nm by a microplate reader (Victor; Perkin Elmer, Turku, Finland).

Determination of ROS Levels

Levels of ROS were measured using 2′7′-dichlorodihydrofluorescein diacetate (H_2DCFDA; Santa Cruz Biotechnology), which is converted to a nonfluorescent derivative (H_2DCF) by intracellular esterases. This molecule can be oxidized by ROS producing intracellular dichlorofluorescein (DCF). The ARPE-19 and hRPE cells were rinsed twice with PBS and incubated with PBS containing 15 μM of H_2DCFDA for 15 minutes at 37°C. Intracellular ROS production was measured by a fluorescence multiplate reader (Victor; Perkin Elmer) with excitation at 485 nm and emission at 530 nm.

Western Blot Analysis

Equal amounts of protein from each sample (35 μg) were measured by SDS-PAGE on 4%–12% gels and electroblotted onto polyvinylidene difluoride membranes (PVDF; Millipore, Billerica, MA, USA). Cells were scraped and lysed with RIPA buffer (Sigma-Aldrich Corp., St. Louis, MO, USA) and protease inhibitor cocktail (Sigma-Aldrich Corp.) for protein extraction. Membranes were incubated overnight at 4°C with rabbit anti-Bax antibody (1:250; Santa Cruz Biotechnology), rabbit anti-Bcl-2 antibody (1:500; Santa Cruz Biotechnology), rabbit anti-CYP2E1 antibody (1:250; Abcam, Cambridge, MA, USA), or mouse anti-β-actin antibody (1:500; Santa Cruz Biotechnology). Finally, membranes were incubated for 2 hours at room temperature with anti-rabbit IgG-HRP (1:10,000; Santa Cruz Biotechnology). Bands were visualized with enhanced chemiluminescence (ECL; Pierce, Thermo Fisher Scientific, Rockford, IL, USA) and detected with Image Quant LAS-4000 mini (GE Healthcare, Uppsala, Sweden). Protein levels were quantified by densitometry using ImageJ software (National Institutes of Health [NIH], Bethesda, MD, USA). Protein expression intensity was corrected by loading control.

Immunocytochemistry

Cells were rinsed twice with PBS and fixed with paraformaldehyde 4% for 10 minutes at room temperature. Cells then were incubated overnight with primary antibody: rabbit anti-CYP2E1 (1:500; Abcam), mouse anti-RPE65 (1:200 Abcam) at 4°C. Thereafter, cells were incubated with fluorescent-conjugated secondary antibodies Alexa Fluor 555 goat anti-rabbit (510–560 nm excitation filter and 590 nm–∞ emission filter), Alexa Fluor 488 goat anti-rabbit or Alexa Fluor 488 goat anti-mouse (482–35 nm excitation filter and 536–40 nm emission filter) (Life Technologies, Thermo Fisher Scientific, Waltham, MA, USA), for 1 hour at room temperature. Finally, for DNA staining, cells were labeled for 10 minutes with 4,6-diamidino-2-phenylindole (DAPI, Sigma-Aldrich Corp.). After slides were rinsed with PBS, a cover slip was placed over the cells before observation under a fluorescence microscope (Eclipse Ti; Nikon, Tokyo, Japan).

RT-PCR and Quantitative RT-PCR

Human RPE tissue, ARPE-19, and HEPG2 cells were incubated in RNA Protect (Qiagen, Hilden, Germany) to attenuate endogenous RNAse activity and mRNA synthesis, and scraped off the plate into a 1.5-mL tube. Cells then were centrifuged at 2500*g* for 10 minutes and the pellet was resuspended in buffer RLT plus (RNeasy Plus Micro/Mini Kits; Qiagen) with 2-mercaptoethanol (1:100; Sigma-Aldrich Corp.). RNA was

Investigative Ophthalmology & Visual Science

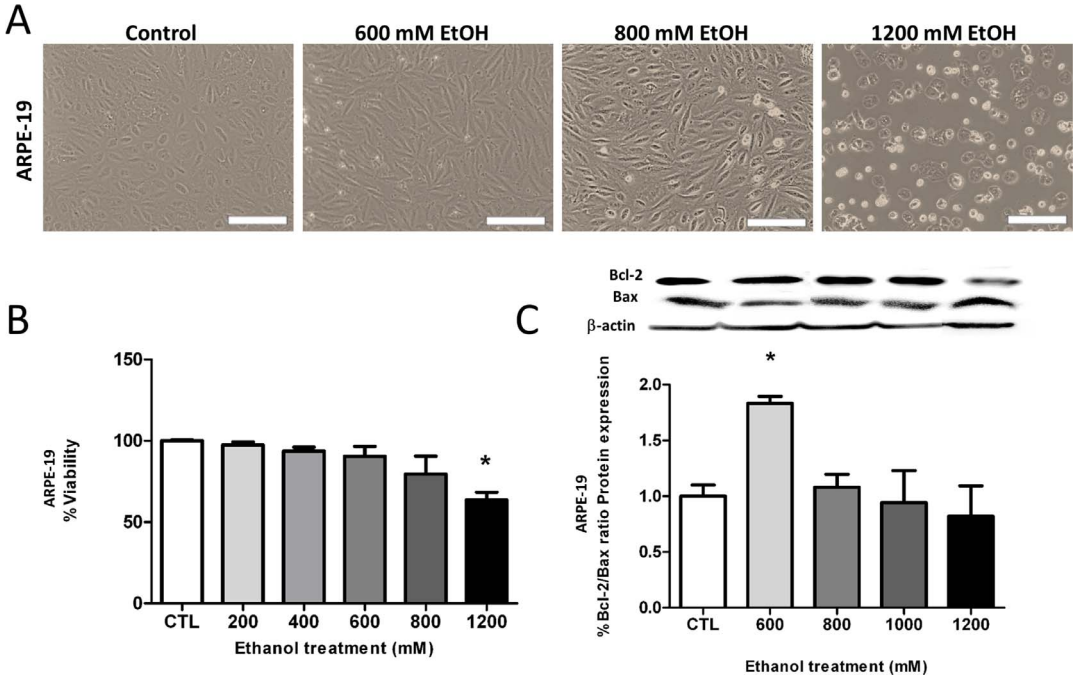

Figure 1. Ethanol promotes changes on ARPE-19 cell viability and morphology. ARPE-19 cell morphology under phase-contrast microscopy after 24 hours of 600, 800, and 1200 mM EtOH exposure (**A**). Cell viability (as XTT assay) on ARPE-19 cells after 24 hours of EtOH treatment (control, 200, 400, 600, 800, and 1200 mM EtOH) (**B**). Semiquantitative analysis of Bcl-2 and Bax proteins by western after 24 hours of treatment with EtOH (control, 200, 400, 600, 800, 1000, and 1200 mM). The Bcl-2/Bax ratio is represented (**C**). Values are expressed as mean ± SEM ($N = 3$). A 1-way ANOVA test and Student's *t*-test analysis were performed (significance level was set at $^*P < 0.05$). Protein expression of CYP2E1 was normalized using β-Actin. *Scale bars*: 100 μm.

harvested from the cells according to manufacturer's protocol (RNeasy Micro/Mini Kits; Qiagen). Reverse transcription-polymerase chain reactions (RT-PCR) were performed with SuperScript III First-Strand Synthesis System (Life Technologies, Thermo Fisher Scientific) and subsequent PCR products were run on 2% agarose gels. Gene-specific primers were obtained from published sequences: β-Actin (F: CAT GTA CGT TGC TAT CCA GGC; R: CTC CTT AAT GTC ACG CAC GAT), CREBBP (F: GAG AGC AAG CAA ACG GAG AG; R: AAG GGA GGC AAA CAG GACA),[42] CYP2E1 (F: CCT ACA TGG ATG CTG TGG TG; R: TGG GGA TGA GGT ATC CTC TG).[40] For quantitative real-time PCRs (qRT-PCR), reactions were performed with Sybr Green Supermix (Applied Biosystems, Carlsbad, CA, USA) and a LightCycler 480 II (Roche). Reactions of RT-PCR were run at either 30 or 35 cycles, and all qRT-PCRs reactions were run at 40 cycles. Quantitative PCR samples were run in triplicate and, in all cases, expression levels were normalized using two housekeeping genes: *β-Actin* and *CREBBP*. The geometric mean of both reference genes was used to standardize the results.

Microsome Isolation

Microsomes of ARPE-19 were prepared with minor modifications as described previously.[43] Briefly, 0.05 g of cells were homogenized in 100 μL homogenization buffer (100 mM Tris-HCl buffer, pH = 7.5, 5 mM KCl, 1 mM DTT, 10 mM EDTA, 5% glycerol, 25% sucrose, and protease inhibitor cocktail; Roche). First, the homogenate was centrifuged at 600*g* for 3 minutes at 4°C, in a Sorvall Legend micro 21 centrifuge (Thermo Scientific, Langenselbold, Germany). The supernatant was transferred carefully to clean centrifuge tubes, diluted 2-fold with distilled water, and centrifuged again at 21,000*g* for 2 hours at 4°C. The pellet was washed in 150 μL of buffer (20 mM Tris-HCl, 5 mM EDTA and protease inhibitor cocktail; Roche) and centrifuged once more at 21,000*g* for 45 minutes at 4°C. The pellet then was resuspended in 100 μL of activity assay buffer and stored at –80°C until further use.

Activity Assay

Activity assay of CYP2E1 was determined by quantification of 4-nitrocatechol (4NC) formation.[44] Preliminary experiments were conducted to determine linear metabolite formation kinetics with respect to time and microsomal protein concentration. Microsomal incubation mixtures consisted of 100 μM p-nitrophenol (PNP; Acros Organics, Thermo Fisher, Morris Plains, NJ, USA), 50 mM potassium phosphate buffer (pH = 6.8; activity assay buffer), cofactor-generating system (1.3 mM NADP, 3.3 mM D-glucose-phosphate, 3.3 mM $MgCl_2$; $4x10^{-4}$ U D-glucose-6-phosphate dehydrogenase in 0.05 mM sodium citrate), and 2 mg of microsomal protein in activity assay buffer at final volume of 0.5 mL. After a preincubation period of 1 minute at 37°C, the reaction was started by addition of microsomal protein and incubated at 37°C for 4 hours in a Thermomixer comfort (Eppendorf, Hamburg, Germany). The reaction was finished by addition of 20% ice-cold trichloracetic acid (TCA) and centrifuged at 10,000*g* for 5 minutes at 4°C. Metabolite formation rate was calculated using known concentrations of 4NC (Acros Organics, Thermo Fisher) as calibration standards (0–1000 nM) and dividing the amount of the metabolite formed by the incubation time and microsomal protein content (nmol/min.mg). The quantification of the metabolite formed was assayed by HPLC using a 1200 series chromatographic system (Agilent Technologies, Santa Clara, CA, USA) equipped with a quaternary pump, automatic injection system, and a DAD UV-Vis detector. A Zorbax Eclipse Plus C-18 column (4.6 × 150 mm, 3.5 μm particle size; Agilent Technologies) was used, operated at room temperature. Experimental conditions were based on previous reports.[45,46] Absorbance was monitored at 334 nm. The mobile phase,

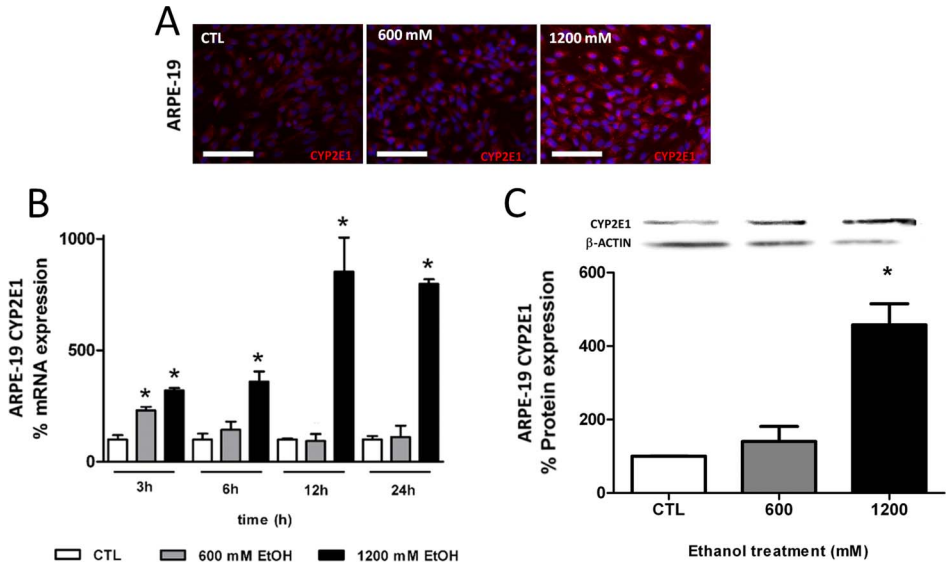

FIGURE 2. Expression of CYP2E1 mRNA and protein levels in ARPE-19 cells after EtOH exposure. Cytochrome p450 2E1 IF in control ARPE-19 cells (CTL) and EtOH-treated cells (600 mM and 1200 mM) with intense cytoplasmic labeling 24 hours after EtOH exposure (**A**). Ethanol exposure of 24 hours increased CYP2E1 mRNA expression in a time-course and concentration-dependent manner (**B**). Expression of CYP2E1 protein was significantly increased after 24 hours of 1200 mM EtOH exposure. Values are expressed as mean ± SEM ($N = 3$). A 1-way ANOVA test and Student's *t*-test analysis were performed (significance level was set at $^*P < 0.05$). Gene expression of *CYP2E1* was normalized by β-Actin and CREBBP. Protein CYP2E1expression was normalized by β-Actin. *Scale bars*: 100 μm.

delivered at a flow rate of 1.5 mL min^{-1}, consisted of 25% ACN, 0.1% TCA, and 74.9% Milli-Q water. The injection volume was 100 μL, the retention time for PNP was 3.27 minutes. The total running time was 8 minutes.

Statistical Analysis

Statistical analyses were performed by using Prism 5.04 software (GraphPad, San Diego, CA, USA), by means of 1- and 2-way ANOVA, and Student's *t*-test. Statistically significant differences were set at $P < 0.05$. Results were obtained from three independent experiments.

RESULTS

EtOH Reduced ARPE-19 Cell Viability

ARPE-19 cells are known to be very resistant to oxidative stress.[47] Thus, the first goal was to establish the EtOH concentration at which cell viability began to be altered. It has been demonstrated previously that ARPE-19 cells require high concentrations of EtOH to be altered.[14] This report states that ARPE-19 cell viability remains unaltered at concentrations below 600 mM EtOH. ARPE-19 cells presented the typical ARPE-19 cell morphology under control conditions (Fig. 1A), while 600 mM

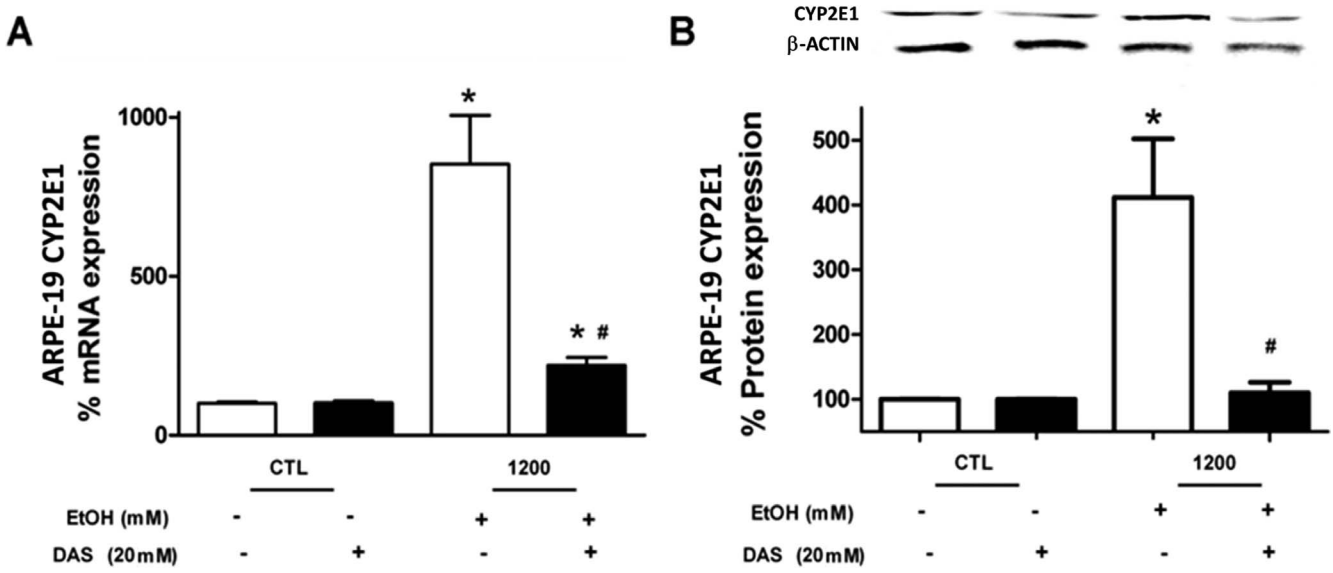

FIGURE 3. Diallyl sulfide reduced CYP2E1 mRNA and protein expression. Diallyl sulfide at 20 mM inhibited EtOH-induced CYP2E1 mRNA expression to control levels (**A**). Ethanol-induced CYP2E1 protein expression also was reduced after 20 mM DAS (**B**). Gene expression of *CYP2E1* was normalized by β-Actin and *CREBBP* gene expression. Protein expression was normalized by β-Actin. A 1-way ANOVA test and Student's *t*-test analysis were performed (significance level was set at $^*P < 0.05$; $^*P < 0.05$ versus control; $\#P < 0.05$ vs. 1200 mM EtOH).

EtOH-treated cells exhibit light morphological changes on cell refringency (Fig. 1A). However, evident morphological alterations are present at 800 mM EtOH. More dramatic changes in shape; refringency, and plate detachment are demonstrated in 1200 mM EtOH-treated cells. All these features typically are related to cell death-damage (Fig. 1A). Using a cell viability assay (XTT), a significant reduction of cell survival at 1200 mM EtOH was confirmed in ARPE-19 cells (Fig. 1B). Despite no differences in cell viability at 600 and 800 mM EtOH, the Bcl-2/Bax ratio was significantly increased from control values at 600 mM EtOH (suggesting prosurvival). Contrarily, it decreased at 800 mM EtOH (suggesting cell death; Fig. 1C).

CYP2E1 Is Present in ARPE-19 Cells and Is Inducible by EtOH

Expression of CYP2E1 protein was assessed in ARPE-19 cells by immunofluorescence (IF). Immunofluorescence labeling showed sparse cytoplasmic localization of CYP2E1 in ARPE-19 cells under basal conditions; however, 600 and 1200 mM EtOH enhanced CYP2E1 IF-labeling (Fig. 2A).

Quantitative PCR analysis confirmed presence of the CYP2E1 mRNA in ARPE-19 cells. As expected, CYP2E1 mRNA levels remained unaltered under basal conditions (white bars in Fig. 2B), but CYP2E1 mRNA expression was significantly increased after the first 3 hours, after 600 mM EtOH exposure, decreasing 6 hours later to control values. However, 1200 mM EtOH promoted a significant increase of CYP2E1 mRNA expression (8-fold over the control one) after 24 hours of EtOH exposure (black bars in Fig. 2B). Statistically significant differences could be set at 3, 12, and 24 hours after 1200 mM EtOH exposure. This increase in CYP2E1 protein expression also was demonstrated by Western blot showing a statistically significant increase at 1200 mM EtOH (Fig. 2C).

DAS Blocks EtOH-Induced CYP2E1 mRNA/Protein Expression and Decreases Microsomal-CYP2E1 Activity

Ethanol at 1200 mM promoted a significant increase of CYP2E1 mRNA/protein expression in ARPE-19 cells (Figs. 3A, 3B). Interestingly, 20 mM DAS blocked this EtOH-induced CYP2E1 protein expression and decreased the CYP2E1 mRNA overexpression.

Activity of CYP2E1 was assessed by the formation of 4NC in microsomes from ARPE-19 cells (Fig. 4). The lowest 4NC level was detected in control ARPE-19 cells (Fig. 4A). Linear regression between CYP2E1 activity and protein levels of microsomes can be seen in Figure 4A. For basal CYP2E1 activity, measured as PNP hydroxylation activity, 2 mg of microsomes were incubated during 4 hours (Fig. 4B). The lowest basal CYP2E1 activity was almost undetectable after DAS addition. However, a significant increase, more than 2-fold the basal CYP2E1 activity, was observed after 24 hours of 1200 mM EtOH exposure. Interestingly, 20 mM DAS caused a significant decrease on CYP2E1 activity in EtOH-treated cells, though this CYP2E1 activity reduction did not reach the control levels (Fig. 4C).

ROS Production Is Reduced by DAS, Improving Cell Viability Outcome

As described above, EtOH-induced CYP2E1 was significantly inhibited by DAS and this inhibition was accompanied by a significant increase in cell viability (Fig. 5A). Although, the CYP2E1 inhibition produced an enhancement on cell viability, this protective effect did not reach the basal cell

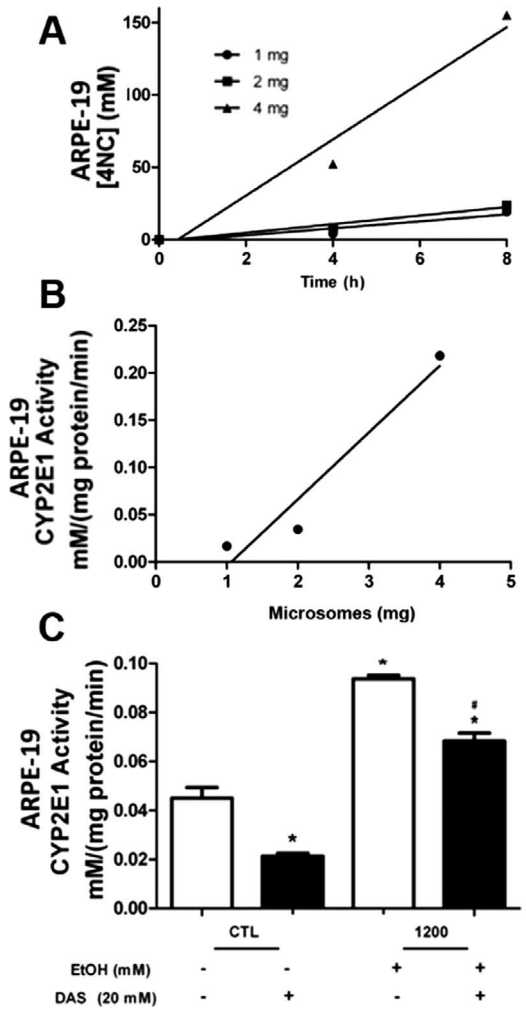

FIGURE 4. Microsomal CYP2E1 activity. Time course of 4NC formation on microsomal-CYP2E1 from ARPE-19 cells (**A**). Graphical representation of the CYP2E1 activity versus different amounts of ARPE-microsomes (along 4 hours, [**B**]). Ethanol-induced CYP2E1 activity and the inhibitory effect of 20 mM DAS (**C**). Values are expressed as mean ± SEM ($N = 3$). A 1-way ANOVA test and Student's *t*-test analysis were performed (significance level was set at $^{*}P < 0.05$; $^{*}P < 0.05$ versus control; $\#P < 0.05$ vs. 1200 mM EtOH). Activity of CYP2E1 was calculated by 4NC formation by the incubation time and microsomal protein content (nmol/min.mg).

viability levels. Formation of ROS was significantly increased in EtOH-treated cells (Fig. 5B). The CYP2E1 inhibition by DAS led to a significant decrease of ROS formation. Under phase-contrast microscopy, 1200 mM EtOH-treated cells presented a clear change in morphology and a more evident refringency than control cells or EtOH + DAS–treated cells (Fig. 5C).

hRPE and ARPE-19 Cells Present Similar Responses to EtOH Exposure

The CYP2E1 mRNA is expressed in ARPE-19 and hRPE cells; CYP2E1 mRNA from HepG2 was used as positive control for CYP2E1 mRNA expression (Fig. 6A). The same gene-specific primer for CYP2E1 recognizes all the studied CYP2E1 mRNA forms (ARPE-19, HepG2, and hRPE) indicating the same genetic profile.

To confirm the identity of hRPE cells we found that human primary RPE culture showed positive immunocytochemical

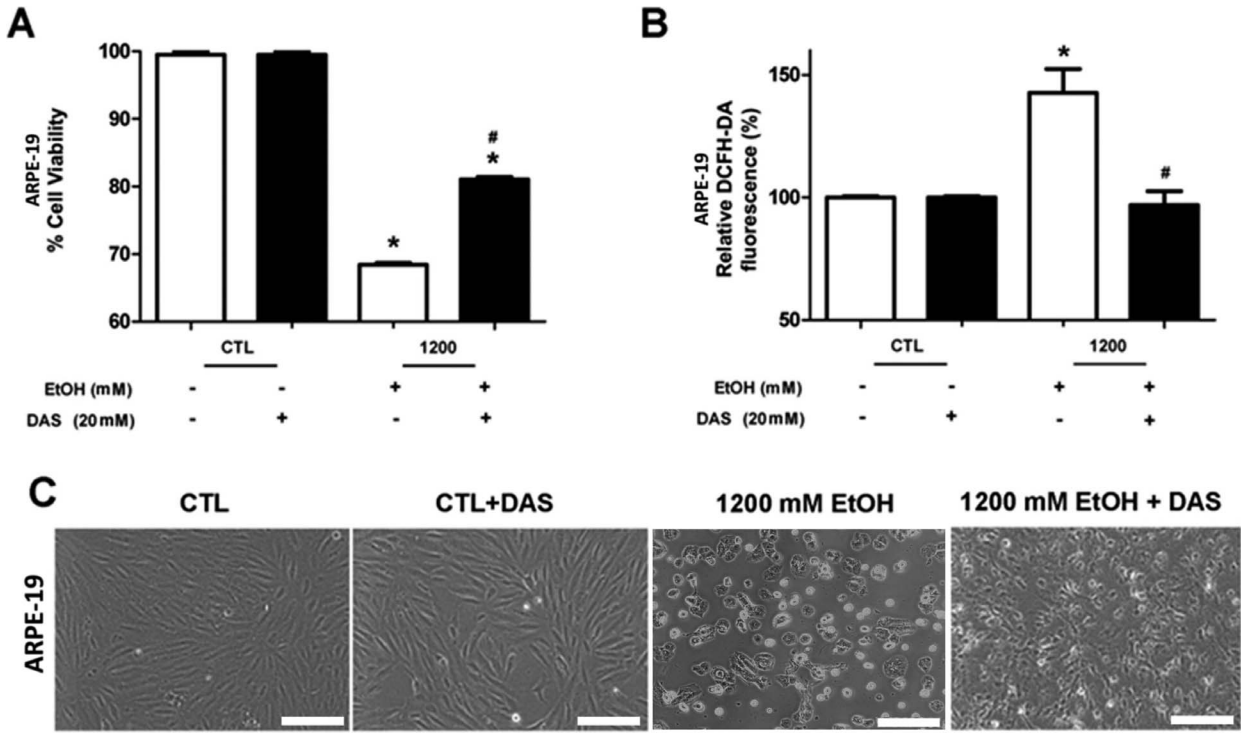

FIGURE 5. Cytochrome p450 2E1 is involved in EtOH-induced oxidative stress in ARPE-19 cells. Diallyl sulfide inhibits the EtOH-induced cell viability loss observed at 1200 mM EtOH (**A**). Additionally, DAS inhibits the EtOH-induced ROS production (as DCFH-DA fluorescence) at 1200 mM EtOH (**B**). Phase-contrast microscopy images of ARPE-19 cells morphology after 24 hours of 1200 mM EtOH exposure and DAS treatment (**C**). Values are expressed as mean ± SEM ($N = 3$). A 1-way ANOVA test and Student's *t*-test analysis were performed (significance level was set at $^*P < 0.05$; $^*P < 0.05$ versus control; $\#P < 0.05$ vs. 1200 mM EtOH). *Scale bar*: 100 μm.

staining for RPE65. Expression of CYP2E1 protein was assessed in hRPE cells (Fig. 6B); CYP2E1-IFC showed a sparse cytoplasmic location in hRPE cells under basal conditions and more evident CYP2E1-positive cells were present after 1200 mM EtOH exposure. Notably, 20 mM DAS reduced the number of CYP2E1–positive cells (Fig. 6D).

One difference between hRPE and ARPE-19 cells relates to the apparent sensitivity to EtOH observed in hRPE. Ethanol at 400 mM already produced significant reductions in hRPE cell viability, whereas ARPE-19 cell viability remained unaltered even at 800 mM EtOH. In both cases, 1200 mM EtOH led to 40% cell death (Fig. 6C).

Ethanol-induced ROS formation also was demonstrated in hRPE cells. Similarly, DAS was able to block this EtOH-dependent ROS formation (Fig. 6E). Furthermore, and stressing this fact, EtOH exposure promoted CYP2E1 expression in ARPE-19/hRPE cells and this increase was blocked by the addition of a selective CYP2E1 inhibitor.

DISCUSSION

To confirm the idea of a local EtOH-metabolism in RPE, the main goal of this report was to find the CYP2E1 enzyme in ARPE-19 and hRPE cells. This is the first report, to our knowledge, confirming the presence of CYP2E1 mRNA in hRPE, previously identified in ARPE-19 cells.[32] Due to the obvious difficulties to obtain hRPE from donors, the present work has been performed mostly on ARPE-19 cells as a model to assess the direct effects of EtOH on RPE (apart from the hepatic metabolism). Considering that RPE is placed in the outermost part of the eye cup, between photoreceptors and blood stream, circulating EtOH may first reach this cell layer. Consequently, the finding of an EtOH-inducible CYP2E1 isoform in RPE elicits great interest in view of the high and continuous levels of EtOH that can be found in human bloodstream, which may reach the eye and could affect RPE and eventually the retina.

Ethanol represents an oxidative insult for cells. In agreement with Brossas et al.,[48] 1200 mM EtOH exerts deleterious effects in ARPE-19 and hRPE cells. Surprisingly, hRPE cells show significant changes on cell viability already at 400 mM EtOH. This suggests that hRPE is more susceptible to EtOH than ARPE-19 cells, where significant cellular changes are present at 600 mM EtOH. As noted by Flores-Bellver et al.[14] and Bonet-Ponce et al.,[49] sublethal EtOH concentrations (600 mM EtOH) promote cellular alterations in terms of mitophagy and protein aggregation in ARPE-19 cells. Interestingly, this autophagic response seems to be related to cell protection.[14] The finding that hRPE cells are more sensitive to EtOH than ARPE-19 cells confirms that ARPE-19 cells are very resistant to oxidative stress.[47,48] Although ARPE-19 cells preserve structural and functional characteristics of RPE, cellular modifications in this cell line may explain this difference in terms of oxidative stress resistance. Interestingly, 100 mM EtOH promotes cell damage in an astrocytic cell line SVGA,[50] whereas 400 to 600 mM EtOH levels are needed in hRPE and ARPE-19, respectively, to decrease cell viability. Probably, the fact that hRPE and ARPE-19 constitutively express ADH[51,52] and CYP2E1 might explain their resistance against xenobiotics and toxic agents, in this case EtOH.

It is of relevance, that 600 mM EtOH increases CYP2E1 mRNA expression in the first 3 hour after EtOH exposure and decrease 3 hours afterwards. This fact fits with data in Figure 1, suggesting that weak or moderate CYP2E1 overexpression could be related to a detoxifying-protective role. Whereas, maintained CYP2E1 overexpression (1200 mM EtOH) could be

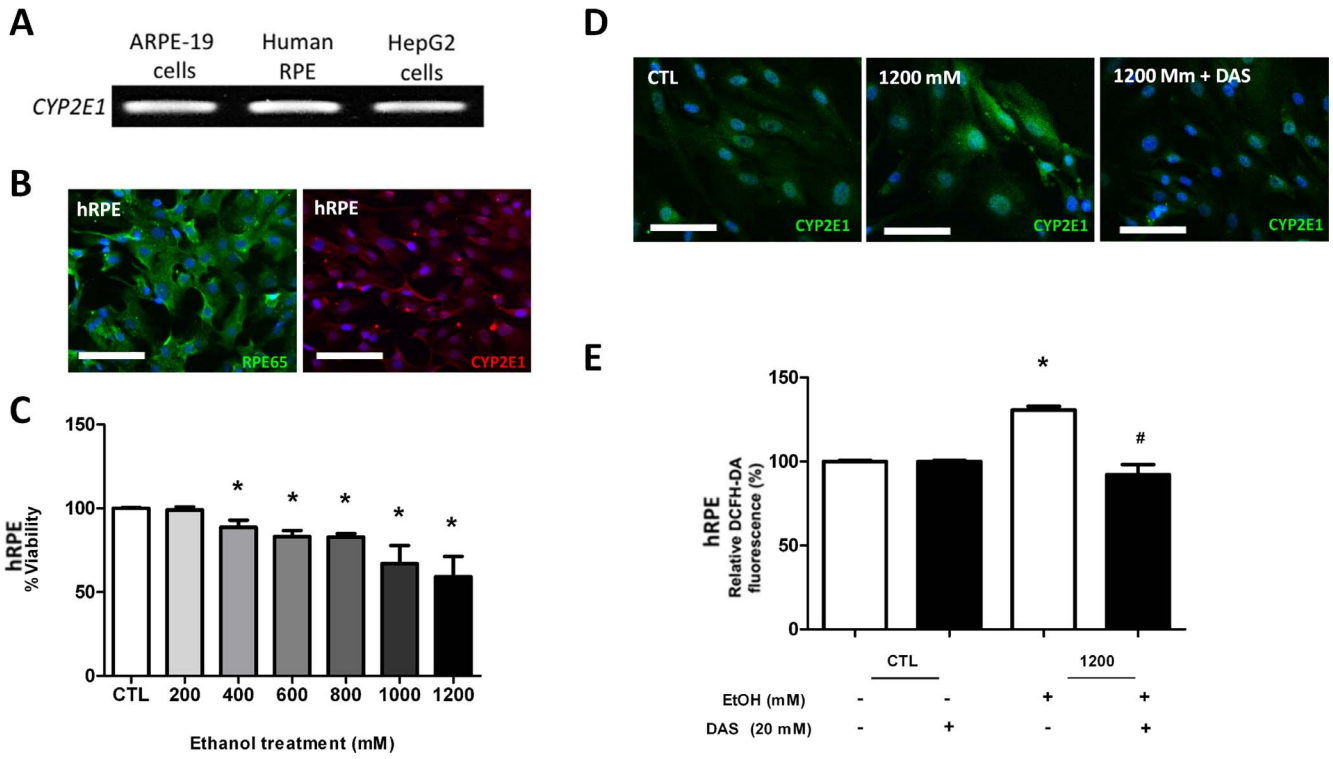

FIGURE 6. Human RPE cells express CYP2E1. The same gene-specific primer recognized CYP2E1 mRNA in ARPE-19 cells, hRPE, and HEPG2 cells (**A**). RPE-65 and CYP2E1 IF on hRPE cells (**B**). Human RPE cell viability (XTT assay) at different EtOH concentrations (control, 200, 400, 600, 800, 1000, and 1200 mM EtOH along 24 hours of exposure) (**C**). Immunofluorescence of CYP2E1 on hRPE cells after 24 hours of 1200 mM EtOH exposure and DAS treatment (**D**). Inhibitory effect of DAS on EtOH-induced ROS production in hRPE cells (DCFH-DA fluorescence [**E**]). Values are expressed as mean ± SEM ($N = 3$). A 1-way ANOVA test and Student's *t*-test analysis were performed (significance level was set at $^*P < 0.05$; $^*P < 0.05$ versus control; $\#P < 0.05$ vs. 1200 mM EtOH). *Scale bars*: 100 μm.

associated with EtOH-induced cellular toxicity. Furthermore, the increased Bcl-2/Bax ratio, the unapparent morphological cellular changes, and the lack of CYP2E1 induction (at 600 mM EtOH) may well fit with our previous data indicating that 600 mM EtOH promotes protective autophagy/mitophagy responses in ARPE-19 cells.[14,49]

The presence of CYP2E1 (herein) and ADH[53,54] in ARPE-19 and hRPE cells strongly supports the proposal of a direct EtOH metabolism in RPE. Cytochrome p450 2E1 represents the major ethanol detoxifying isoform that furthermore is induced by EtOH, but paradoxically it is poorly expressed in ARPE-19 cells in basal conditions.[32] The goal of the present work was addressed to resolve this issue. In agreement with Badger et al.,[21] who reported hepatic CYP2E1 induction by EtOH, in ARPE-19 cells CYP2E1 mRNA expression was increased in a fast, progressive and maintained manner after EtOH exposure (600–1200 mM).

A competitive inhibitor of CYP2E1, DAS blocks ROS production by direct molecular interaction and indirectly by inhibiting CYP2E1 transcription.[50] The results herein indicated that DAS reduces ROS and CYP2E1 protein/mRNA levels in ARPE-19 cells. In agreement with this, it has been described that *CYP2E1* gene transcription is ROS-mediated and consequently, CYP2E1 induction is accompanied by additional ROS production enhancing *CYP2E1* transcription.[50]

Recent findings from our group indicate that low EtOH concentrations are able to raise autophagy flux in ARPE-19 cells demonstrating a protective role of autophagy against EtOH exposure[49] in agreement with Chen et al.,[55] who indicated the protective role of autophagy against EtOH exposure. Furthermore, EtOH influence also is associated with protein aggregation depending on the generation of 4-hydroxy-nonenal (a lipid peroxidation product) and such "aggresomes" appear in ARPE-19 cells.[14] In contrast with this, CYP2E1-derived ROS have been related directly to the inhibition of autophagy in liver, using a binge model of EtOH exposure in hepatic cell lines.[56] This apparent discrepancy can be attributed not only to the different experimental model used, but also to the type of treatment and the EtOH concentrations used. Plausibly, EtOH-derived ROS are produced in a dose-dependent manner leading to different autophagy related phenomena: from cell protection to cell death. In any case, the observed CYP2E1 induction by EtOH in ARPE-19 cells fits with the increase of ROS production at different EtOH concentrations and the reversion of this phenomenon by the addition of DAS.

Some epidemiological data support the suggestion that EtOH may affect the retina.[57,58] Fitting with this, electroretinograms recorded from chronic EtOH-treated rats showed that the b-wave amplitude was significantly diminished. B-wave amplitude is attributable to depolarizing bipolar cell activity and Müller cells. Interestingly, this alteration was accompanied by a marked increase of the antiapoptotic protein Bcl-2 in Müller cells.[12] The protein Bcl-2 is an antiapoptotic protein related to antioxidant pathways,[59] so this increase could be attributable to EtOH-induced oxidative stress. In fact, the administration of Ebselen prevented this EtOH-induced b-wave impairment.[13] Additionally, EtOH and lipid peroxidation metabolites inhibit the conversion of all-*trans*-retinol to all-*trans*-retinal[60] affecting visual cycle. Although some questions still are unresolved, it seems clear that oxidative stress has a central role in those EtOH-related retinal alterations. Future studies might be addressed to confirm the primary role of RPE on this EtOH-induced phenomenon.

One limitation of this study deals with the EtOH concentrations reaching the eye. Most probably, EtOH circulating levels will be lower than the initial concentrations used herein for cell cultures. Additionally, the presence of the choriocapillaris will affect the actual EtOH concentration finally reaching the eye. In this line, it is very interesting to note that vitreal EtOH levels are higher than those obtained from blood,[61] so it seems reliable that EtOH reaches the eye. As previously reported, 40 Mm EtOH circulating blood levels significantly affected rat retina.[6,8,12,13] These EtOH levels are much lower than those used initially herein for cell cultures (600 mM). Obviously, vaporization of EtOH in cultures is a significant phenomenon affecting the final EtOH concentration and, therefore, it is extremely difficult to confirm the actual EtOH concentration reaching the cultured cells.[62]

The presence and activity of CYP2E1 suggests that the RPE has a role on local EtOH metabolism, which is likely protective at low EtOH concentrations, whereas it is deleterious at higher ones. The presence of CYP2E1 in hRPE and ARPE-19 cells reinforces the protective role of the RPE and strongly suggests additional roles for CYP2E1 related to vision.

Acknowledgments

Supported partially by funds from Fundación Universidad Católica de Valencia 'San Vicente Mártir', Valencia, Spain, and Conselleria de Educació, Cultura i Sport, Valencia, Spain.

Disclosure: **N. Martinez-Gil**, None; **M. Flores-Bellver**, None; **S. Atienzar-Aroca**, None; **D. Lopez-Malo**, None; **A.C. Urdaneta**, None; **J. Sancho-Pelluz**, None; **C. Peris-Martínez**, None; **L. Bonet-Ponce**, None; **F.J. Romero**, None; **J.M. Barcia**, None

References

1. Caro AA, Cederbaum AI. Oxidative stress, toxicology, and pharmacology of CYP2E1. *Ann Rev Pharmacol Toxicol*. 2004; 44:27–42.
2. Ekstrom G, Ingelman-Sundberg M. Rat liver microsomal NADPH-supported oxidase activity and lipid peroxidation dependent on ethanol-inducible cytochrome P-450 (P-450IIE1). *Biochem Pharmacol*. 1989;38:1313–1319.
3. Persson JO, Terelius Y, Ingelman-Sundberg M. Cytochrome P-450-dependent formation of reactive oxygen radicals: isozyme-specific inhibition of P-450-mediated reduction of oxygen and carbon tetrachloride. *Xenobiotica*. 1990;20:887–900.
4. Albano E, Clot P, Morimoto M, Tomasi A, Ingelman-Sundberg M, French SW. Role of cytochrome P4502E1-dependent formation of hydroxyethyl free radical in the development of liver damage in rats intragastrically fed with ethanol. *Hepatology*. 1996;23:155–163.
5. Fadda F, Rossetti ZL. Chronic ethanol consumption: from neuroadaptation to neurodegeneration. *Prog Neurobiol*. 1998; 56:385–431.
6. Johnsen-Soriano S, Bosch-Morell F, Miranda M, et al. Ebselen prevents chronic alcohol-induced rat hippocampal stress and functional impairment. *Alcohol Clin Exp Res*. 2007;31:486–492.
7. Bondy SC, Guo SX. Regional selectivity in ethanol-induced pro-oxidant events within the brain. *Biochem Pharmacol*. 1995; 49:69–72.
8. Bosch-Morell F, Martinez-Soriano F, Colell A, Fernandez-Checa JC, Romero FJ. Chronic ethanol feeding induces cellular antioxidants decrease and oxidative stress in rat peripheral nerves. Effect of S-adenosyl-L-methionine and N-acetyl-L-cysteine. *Free Rad Biol Med*. 1998;25:365–368.
9. Ramachandran V, Watts LT, Maffi SK, Chen J, Schenker S, Henderson G. Ethanol-induced oxidative stress precedes mitochondrially mediated apoptotic death of cultured fetal cortical neurons. *J Neurosci Res*. 2003;74:577–588.
10. Sun AY, Chen YM, James-Kracke M, Wixom P, Cheng Y. Ethanol-induced cell death by lipid peroxidation in PC12 cells. *Neurochem Res*. 1997;22:1187–1192.
11. Laposata M. Assessment of ethanol intake. Current tests and new assays on the horizon. *Am J Clin Path*. 1999;112:443–450.
12. Sancho-Tello M, Muriach M, Barcia J, et al. Chronic alcohol feeding induces biochemical, histological, and functional alterations in rat retina. *Alcohol Alcohol*. 2008;43:254–260.
13. Johnsen-Soriano S, Genoves JM, Romero B, et al. Chronic ethanol feeding induces oxidative stress in the rat retina: treatment with the antioxidant ebselen. *Arch Soc Esp Oftalmol*. 2007;82:757–762.
14. Flores-Bellver M, Bonet-Ponce L, Barcia JM, et al. Autophagy and mitochondrial alterations in human retinal pigment epithelial cells induced by ethanol: implications of 4-hydroxy-nonenal. *Cell Death Dis*. 2014;5:e1328.
15. Cederbaum AI. Alcohol metabolism. *Clin Liver Dis*. 2012;16: 667–685.
16. Guengerich FP, Kim DH, Iwasaki M. Role of human cytochrome P-450 IIE1 in the oxidation of many low molecular weight cancer suspects. *Chemical Res Toxicol*. 1991;4:168–179.
17. Muller FL, Lustgarten MS, Jang Y, Richardson A, Van Remmen H. Trends in oxidative aging theories. *Free Rad Biol Med*. 2007;43:477–503.
18. Albano E. Oxidative mechanisms in the pathogenesis of alcoholic liver disease. *Mol Asp Med*. 2008;29:9–16.
19. Koop DR, Morgan ET, Tarr GE, Coon MJ. Purification and characterization of a unique isozyme of cytochrome P-450 from liver microsomes of ethanol-treated rabbits. *J Biol Chem*. 1982;257:8472–8480.
20. Lieber CS, DeCarli LM. Hepatic microsomal ethanol-oxidizing system. In vitro characteristics and adaptive properties in vivo. *J Biol Chem*. 1970;245:2505–2512.
21. Badger TM, Huang J, Ronis M, Lumpkin CK. Induction of cytochrome P450 2E1 during chronic ethanol exposure occurs via transcription of the CYP 2E1 gene when blood alcohol concentrations are high. *Biol Biophys Res Comm*. 1993;190:780–785.
22. Miksys SL, Tyndale RF. Drug-metabolizing cytochrome P450s in the brain. *J Psych Neurosci*. 2002;27:406–415.
23. Tsutsumi M, Lasker JM, Takahashi T, Lieber CS. In vivo induction of hepatic P4502E1 by ethanol: role of increased enzyme synthesis. *Arch Biochem Biophys*. 1993;304:209–218.
24. Zimatkin SM, Liopo AV, Deitrich RA. Distribution and kinetics of ethanol metabolism in rat brain. *Alcohol Clin Exp Res*. 1998;22:1623–1627.
25. Strauss O, Stumpff F, Mergler S, Wienrich M, Wiederholt M. The Royal College of Surgeons rat: an animal model for inherited retinal degeneration with a still unknown genetic defect. *Acta Anat*. 1998;162:101–111.
26. Baehr W, Wu SM, Bird AC, Palczewski K. The retinoid cycle and retina disease. *Vision Res*. 2003;43:2957–2958.
27. Besch D, Jagle H, Scholl HP, Seeliger MW, Zrenner E. Inherited multifocal RPE-diseases: mechanisms for local dysfunction in global retinoid cycle gene defects. *Vision Res*. 2003;43:3095–3108.
28. Dornonville de la Cour M. Ion transport in the retinal pigment epithelium. A study with double barrelled ion-selective microelectrodes. *Acta Ophthalmologa Suppl*. 1993; 209:1–32.
29. Steinberg RH. Interactions between the retinal pigment epithelium and the neural retina. *Doc Ophthalmol*. 1985;60: 327–346.

30. Thompson DA, Gal A. Vitamin A metabolism in the retinal pigment epithelium: genes, mutations, and diseases. *Prog Retin Eye Res*. 2003;22:683–703.
31. Steinberg RH, Linsenmeier RA, Griff ER. Three light-evoked responses of the retinal pigment epithelium. *Vision Res*. 1983; 23:1315–1323.
32. Nakano M, Kelly EJ, Wiek C, Hanenberg H, Rettie AE. CYP4V2 in Bietti's crystalline dystrophy: ocular localization, metabolism of omega-3-polyunsaturated fatty acids, and functional deficit of the *P*.H331P variant. *Mol Pharmacol*. 2012;82:679–686.
33. Shichi H, Atlas SA, Nebert DW. Genetically regulated aryl hydrocarbon hydroxylase induction in the eye: possible significance of the drug-metabolizing enzyme system for the retinal pigmented epithelium-choroid. *Exp Eye Res*. 1975;21: 557–567.
34. Shichi H, Tsunematsu Y, Nebert DW. Aryl hydrocarbon hydroxylase induction in retinal pigmented epithelium: possible association of genetic differences in a drug-metabolizing enzyme system with retinal degeneration. *Exp Eye Res*. 1976;23:165–176.
35. Doyle JW, Dowgiert RK, Buzney SM. Retinoic acid metabolism in cultured retinal pigment epithelial cells. *Invest Ophthalmol Vis Sci*. 1995;36:708–717.
36. Nakamura K, Fujiki T, Tamura HO. Age, gender and region-specific differences in drug metabolising enzymes in rat ocular tissues. *Exp Eye Res*. 2005;81:710–715.
37. Driessen CA, Janssen BP, Winkens HJ, van Vugt AH, de Leeuw TL, Janssen JJ. Cloning and expression of a cDNA encoding bovine retinal pigment epithelial 11-cis retinol dehydrogenase. *Invest Ophthalmol Vis Sci*. 1995;36:1988–1996.
38. Jang GF, Van Hooser JP, Kuksa V, et al. Characterization of a dehydrogenase activity responsible for oxidation of 11-cis-retinol in the retinal pigment epithelium of mice with a disrupted RDH5 gene. A model for the human hereditary disease fundus albipunctatus. *J Biol Chem*. 2001;276:32456–32465.
39. Patton WP, Routledge MN, Jones GD, et al. Retinal pigment epithelial cell DNA is damaged by exposure to benzo[a]pyrene, a constituent of cigarette smoke. *Exp Eye Res*. 2002;74: 513–522.
40. Zhang T, Xiang CD, Gale D, Carreiro S, Wu EY, Zhang EY. Drug transporter and cytochrome P450 mRNA expression in human ocular barriers: implications for ocular drug disposition. *Drug Metab Dispos*. 2008;36:1300–1307.
41. Zhu M, Provis, JM Penfold PL. Isolation, culture and characteristics of human foetal and adult retinal pigment epithelium. *Aust N Zeal J Ophthalmol*. 1998;26:50–55.
42. Maruotti J, Wahlin K, Gorrell D, Bhutto I, Lutty G, Zack DJ. A simple and scalable process for the differentiation of retinal pigment epithelium from human pluripotent stem cells. *Stem Cells Translat Med*. 2013;2:341–354.
43. Abas L, Luschnig C. Maximum yields of microsomal-type membranes from small amounts of plant material without requiring ultracentrifugation. *Analyt Biochem*. 2010;401:217–227.
44. Chang TK, Crespi CL, Waxman DJ. Spectrophotometric analysis of human CYP2E1-catalyzed *P*-nitrophenol hydroxylation. *Methods Mol Biol*. 2006;320:127–131.
45. Elbarbry F, Wilby K, Alcorn J. Validation of a HPLC method for the determination of *P*-nitrophenol hydroxylase activity in rat hepatic microsomes. *J Chromatog B Analyt Technol Biomed Life Sci*. 2006;834:199–203.
46. Tassaneeyakul W, Veronese ME, Birkett DJ, Gonzalez FJ, Miners JO. Validation of 4-nitrophenol as an in vitro substrate probe for human liver CYP2E1 using cDNA expression and microsomal kinetic techniques. *Biochem Pharmacol*. 1993; 46:1975–1981.
47. Kurz T, Karlsson M, Brunk UT, Nilsson SE, Frennesson C. ARPE-19 retinal pigment epithelial cells are highly resistant to oxidative stress and exercise strict control over their lysosomal redox-active iron. *Autophagy*. 2009;5:494–501.
48. Brossas JY, Tanguy R, Brignole-Baudouin F, Courtois Y, Torriglia A, Treton J. L-DNase II associated with active process during ethanol induced cell death in ARPE-19. *Mol Vis*. 2004;10:65–73.
49. Bonet-Ponce L, Saez-Atienzar S, da Casa C, et al. On the mechanism underlying ethanol-induced mitochondrial dynamic disruption and autophagy response. *Biochim Biophys Acta*. 2015;7:1400–1409.
50. Jin M, Ande A, Kumar A, Kumar S. Regulation of cytochrome P450 2e1 expression by ethanol: role of oxidative stress-mediated pkc/jnk/sp1 pathway. *Cell Death Dis*. 2013;4:e554.
51. Simon A, Hellman U, Wernstedt C, Eriksson U. The retinal pigment epithelial-specific 11-cis retinol dehydrogenase belongs to the family of short chain alcohol dehydrogenases. *J Biol Chem*. 1995;270:1107–1112.
52. Suzuki Y, Ishiguro S, Tamai M. Identification and immunohistochemistry of retinol dehydrogenase from bovine retinal pigment epithelium. *Biochim Biophys Acta*. 1993;1163:201–208.
53. Martras S, Alvarez R, Martínez SE, et al. The specificity of alcohol dehydrogenase with cis-retinoids. Activity with 11-cis-retinol and localization in retina. *Eur J Biochem*. 2004;271: 1660–1670.
54. Holmes RS, Popp RA, VandeBerg JL. Genetics of ocular NAD+-dependent alcohol dehydrogenase and aldehyde dehydrogenase in the mouse: evidence for genetic identity with stomach isozymes and localization of Adh-4 on chromosome 11 near trembler. *Biochem Genet*. 1988;26:191–205.
55. Chen G, Ke Z, Xu M, et al. Autophagy is a protective response to ethanol neurotoxicity. *Autophagy*. 2012;11:1577–1589.
56. Wu D, Wang X, Zhou R, Yang L, Cederbaum AI. Alcohol steatosis and cytotoxicity: the role of cytochrome P4502E1 and autophagy. *Free Rad Biol Med*. 2012;53:1346–1357.
57. Klein R, Lee KE, Gangnon RE, Klein BE. Relation of smoking, drinking, and physical activity to changes in vision over a 20-year period: the Beaver Dam Eye Study. *Ophthalmology*. 2014; 121:1220–1228.
58. Li Z, Xu K, Wu S, et al. Alcohol consumption and visual impairment in a rural northern chinese population. *Ophthal Epidemiol*. 2014;21:384–390.
59. Hockenbery DM, Oltvai ZN, Yin XM, Milliman CL, Korsmeyer SJ. Bcl-2 functions in an antioxidant pathway to prevent apoptosis. *Cell*. 1993;75:241–251.
60. Khalighi M, Brzezinski MR, Chen H, Juchau MR. Inhibition of human prenatal biosynthesis of all-trans-retinoic acid by ethanol, ethanol metabolites, and products of lipid peroxidation reactions: a possible role for CYP2E1. *Biochem Pharmacol*. 1999;577:811–821.
61. Honey D, Caylor C, Luthi R, Kerrigan S. Comparative alcohol concentrations in blood and vitreous fluid with illustrative case studies. *J Analyt Toxicol*. 2005;29:365–369.
62. Eysseric H, Gonthier B, Soubeyran A, Bessard G, Saxod R, Barret L. There is not simple method to maintain a constant ethanol concentration in long-term cell culture: keys to a solution applied to the survey of astrocytic ethanol absorption. *Alcohol*. 1997;14:111–115.

Investigative Ophthalmology & Visual Science